Phytocannabinoids promote viability and functional adipogenesis of bone marrow-derived mesenchymal stem cells through different molecular targets

Tariq Fellous[a], Fabrizia De Maio[a], Hilal Kalkan[a], Biagio Carannante[a], Serena Boccella[b], Stefania Petrosino[a], Sabatino Maione[b], Vincenzo Di Marzo[a,c,*], Fabio Arturo Iannotti[a,*]

[a] Endocannabinoid Research Group, Institute of Biomolecular Chemistry (ICB), National Research Council (CNR), Pozzuoli (NA) 80078 IT, Italy
[b] Department of Experimental Medicine, Section of Pharmacology L. Donatelli, Università degli Studi della Campania "Luigi Vanvitelli", Naples, Italy
[c] Canada Excellence Research Chair on the Microbiome-Endocannabinoidome Axis in Metabolic Health, Institut Universitaire de Cardiologie et de Pneumologie de Québec and Institut sur la Nutrition et les Aliments Fonctionnels, Université Laval, Quebec City G1V 0A6, Canada

ABSTRACT

The cellular microenvironment plays a critical role in the maintenance of bone marrow-derived mesenchymal stem cells (BM-MSCs) and their subsequent cell lineage differentiation. Recent studies suggested that individuals with adipocyte-related metabolic disorders have altered function and adipogenic potential of adipose stem cell subpopulations, primarily BM-MSCs, increasing the risk of heart attack, stroke or diabetes. In this study, we explored the potential therapeutic effect of some of the most abundant non-euphoric compounds derived from the *Cannabis sativa* plant (or phytocannabinoids) including tetrahydrocannabivarin (THCV), cannabidiol (CBD), cannabigerol (CBG), cannabidiolic acid (CBDA) and cannabigerolic acid (CBGA), by analysing their pharmacological activity on viability of endogenous BM-MSCs as well as their ability to alter BM-MSC proliferation and differentiation into mature adipocytes. We provide evidence that CBD, CBDA, CBGA and THCV (5 μM) increase the number of viable BM-MSCs; whereas only CBG (5 μM) and CBD (5 μM) alone or in combination promote BM-MSCs maturation into adipocytes via distinct molecular mechanisms. These effects were revealed both *in vitro* and *in vivo*. In addition, phytocannabinoids prevented the insulin signalling impairment induced by palmitate in adipocytes differentiated from BM-MSCs. Our study highlights phytocannabinoids as a potential novel pharmacological tool to regain control of functional adipose tissue in unregulated energy homeostasis often occurring in metabolic disorders including type 2 diabetes mellitus (T2DM), aging and lipodystrophy.

1. Introduction

Adipose tissue not only sequesters and stores excess energy, but it is also a metabolic endocrine organ that secretes adipokines (adiponectin and leptin), growth factors and cytokines, which collectively modulate systemic energy balance. Adipose tissue normally grows by two mechanisms: hyperplasia (increase in adipocyte number) and hypertrophy (increase in adipocye size). The alteration of either mechanism may lead to inadequate energy storage capacity, and perturbation of glucose and lipid homeostasis [1]. This can result in acquired insulin resistance, abnormal insulin secretion, inflammation, hyperlipidemia and hyperglycemia, all factors that link dysfunctional adipogenesis with numerous metabolic pathophysiologies [1]. Bone marrow mesenchymal stem cells (BM-MSCs) represent a population of non-hematopoietic stromal cells showing a fibroblast-like morphology with multi-lineage cell differentiation potential, including osteoblasts, chondrocytes, skeletal muscle and adipocytes. MSCs can also be found within adipose tissue, connective tissues, peripheral blood, lung and neonatal tissues such as placenta and umbilical cord [2–7]. In a healthy state, BM-MSCs differentiate and mobilize to repopulate damaged tissues, including peripheral adipose tissue. This significantly contributes to systemic adipogenesis, providing long-term regenerative capacity [8–10], and thus eliciting hope for therapeutic interventions targeting adipocyte dysfunction. In this regard, MSC-based transplantation therapies have shown promise for relieving symptoms of obesity, diabetes, and neurological, inflammatory and auto-immune diseases [11–15]. Unfortunately, however, the heterogeneity, senescence, efficacy, safety and alterations in phenotype during long-term culture of exogenous MSCs are problematic and often lead to failure [16].

The Endocannabinoid System (ECS) refers to a large group of

molecules that in our body control the activity of the two major cannabinoid lipid-mediators named Anandamide (AEA) and 2-Arachidonoylglycerol (2-AG). Since their discovery, it appeared clear that both AEA and 2-AG play an important role in preserving the health of our organism. As a consequence, alterations in the activity of AEA and 2-AG have been described in a plethora of disorders affecting both the central nervous system as well as peripheral organs and tissues [17,18]. The ECS in adipocytes has been reported to regulate the thermogenic function by controlling the activity of the white and brown adipose tissues (WAT and BAT) through the activation of the cannabinoid receptors called CB_1 and CB_2 [19], Of note, endocannabinoid tone in adipocytes is subject to negative feed-back control by the peroxisome proliferator-activated receptor gamma (PPARγ) [20,21], which has been suggested to be a target of both anandamide and some metabolites of 2-AG [22]. However, obesity desensitizes this process leading to reduced insulin sensitivity and negatively affecting glucose and lipid metabolism. This leads to a self-perpetuating overstimulation of the ECS, contributing to reduced energy expenditure, adipocyte hypertrophy and inflammation-related β-cell loss [23–26]. As adipocyte precursors, MSCs express all the components of the ECS [27]; accordingly, CB_1 and CB_2 activity can regulate their migration, survival and differentiation [28–31].

Interestingly, the phytocannabinoids, which encompass a large class of compounds identified and isolated from *Cannabis sativa*, have been proposed to interact with a variety of molecular targets that include, but are not limited to, CB_1 and CB_2 receptors, which can be directly activated or antagonised at physiologically achievable concentrations (in the nM range) by Δ^9-tetrahydrocannabinol (THC) and Δ^9-tetrahydrocannabivarin (THCV), respectively [32–34]. Also, phytocannabinoids have other ways of potentially and indirectly modifying, although at low micromolar concentrations, the activity of ECS enzymes or non-cannabinoid receptors, such as the nuclear receptor superfamily PPARs (α, δ and γ) [22,29,35], which are key regulators of adipogenesis, lipid metabolism and glucose metabolism. By acting at these different targets, including metabotropic or intracellular receptors belonging or somehow related to the ECS, phytocannabinoids exert neuroprotective as well as anti-inflammatory actions *in vivo* [36–39]. Among the phytocannabinoids, Δ^9-THC is the best known due to its CB_1-mediated euphoric properties; however other compounds of interest include THCV, cannabidiol (CBD), cannabigerol (CBG), cannabidiolic acid (CBDA) and cannabigerolic acid (CBGA). Previous studies have shown that phytocannabinoid treatment, most notably THCV, increases murine BM-MSC colony formation with a committed osteogenic differentiation potential, mediated by CB_2 activity [40]. CBD (3 µM) promoted *ex vivo* MSC migration and osteoblastic differentiation in a manner reversed by AM630 (CB_2 antagonist) or O-1602 (a GPR55 agonist), leading the authors to suggest that these effects were mediated by CB2 activation or GPR55 inactivation; however, neither AM630 or O-1602 were tested on their own, and therefore caution must be applied in the interpretation of these data [41], particularly as CBD has also been suggested to restore adipogenic and chondrogenic *in vitro* differentiation capacity via PPARγ in debilitated MSCs with an induced inflammatory phenotype [35]. Finally, a 3 µM concentration of CBD, and its analogue CBDV, promoted the maturation of mesenchymal derived skeletal muscle precursors cells into functional myotubes in healthy and pathological conditions such as Duchenne's muscular dystrophy [42].

In several pathophysiologies associated with adipose tissue dysfunction, such as obesity and aging, BM-MSCs become exhausted and depleted with reduced function and differentiation potential due to increased senescence, which leads to concomitant pathologies *e.g.* type 2 diabetes (T2D) or lipodystrophy. In these cases, enhancement in the number of viable BM-MSCs as well as reinstating functional and requisite endogenous adipogenesis is considered to be beneficial [43–45]. Consequently, in this study we investigated the *in vitro* and *in vivo* pharmacological effect of several phytocannabinoids, including CBD, CBDA, CBG, CBGA and THCV, alone or combination, on murine BM-

MSC viability, adipocyte lineage commitment, adipocyte differentiation efficacy and the ability to promote a mature functional adipocyte phenotype.

2. Materials and methods

2.1. Bone marrow fibroblast colony-forming unit (CFU-F) assay

Whole bone marrow cells extracted from the hind limb femurs of naive female C57BL/6 mice of 6 weeks of age (16–18 g; Harlan Laboratories, Italy) were added to tissue culture treated 6-well plates containing 3 ml of complete MesenCult™ Medium (05502; StemCell Technologies) at a cell density of 5×10^5 cells per well to select for CFU-Fs. Specified treatments were added to the relevant wells. These cells were incubated at 37 °C under 5% CO_2. A fresh half medium change was performed after 7 days, and returned to the incubator until stromal colonies appeared (> 20 cells/colony). This takes approximately an additional 7 days (*i.e.* 14 days in total). The colonies were fixed in methanol, stained (Giemsa), enumerated and quantified.

2.2. Primary mesenchymal stem cells (MSCs)

Primary bone marrow MSCs were derived and expanded directly from early stage CFU-F colonies, after 7 days in culture the colonies were passaged by treating them with 0.25% trypsin/0.02% EDTA (Gibco) at 37 °C under 5% CO_2. The detached cells were collected within 3 min ready for subculture, and plated at a density of 1000 cells/cm^2 in standard growth media (DMEM low glucose), cat. D6046 Life Technologies, Milan IT) supplemented with 10% FBS (cat. 10270106 Life Technologies, Milan IT) and 1% Pen/Strep (cat. 1514022 Life Technologies, Milan IT). Fresh media was replaced every 3 days, and subsequent passaging was performed under the same conditions, the cells were maintained at sub-confluence for between 3 and 10 passages. Cells were allowed to reach 90% confluence prior to experimental treatments. Additionally, the plastic adherent cells that comprise bone marrow CFU-Fs were characterised after expansion, assessing for MSC lineage markers by qPCR and trilineage MSC differentiation capacity.

2.3. Mesenchymal stem cell trilineage differentiation

To test for MSC trilineage differentiation capacity putative MSCs were cultured in either adipogenic, osteogenic or chondrogenic differentiation media. (a) Adipogenic differentiation: Six well-plates containing 90% confluent primary MSCs (passage 3–10) were cultured in 3 ml of standard growth media DMEM low glucose supplemented with 20% FBS (cat. 10270106 Life Technologies, Milan IT), Pen/Strep 1% (cat. 1514022 Life Technologies, Milan IT), supplemented with insulin 1ug/ml, dexamethazone 250 nM (cat. D1756; Sigma-Aldrich Milan Italy), 3-isobutyl-1-methylxanthine (IBMX) 500 µM (cat. I7018; Sigma-Aldrich Milan Italy) and indomethacin 10 µM (cat. I7378; Sigma-Aldrich Milan Italy). The media was changed for fresh differentiation media every 3–4 days for 2–3 weeks. (b) Osteogenic differentiation: Six well-plates containing 90% confluent primary MSCs (passage 3–10) were cultured in 3 ml of standard growth media DMEM supplemented with 10% FBS, Pen/Strep 1%, β-Glycerol Phosphate 20 µM, ascorbic acid 2-phosphate 50 µg/ml and dexamethazone 10 nM (cat. D1756; Sigma-Aldrich Milan Italy). The media was changed for fresh differentiation media every 3–4 days for 2–3 weeks. (c) Chondrogenic differentiation: Six well plates containing 90% confluent primary MSCs (passage 3–10) were cultured in 3 ml of serum free standard growth media DMEM supplemented with Pen Strep 1%, TGFβ1 10 ng/ml, dexamethazone 0.1 µM, L-Proline 40 µg/ml, BSA 1.25 mg/ml, Sodium Pyruvate 100 µg/ml, $1 \times$ ITS + 3 5 µg/ml. The media was changed for fresh differentiation media every 3–4 days for 3–4 weeks. Cells were then stained with Oil Red O, Alizarin Red S and Alcian Blue for adipocytes, osteoblasts and chondrocytes, respectively.

2.4. Quantification of intracellular triglyceride levels

Confluent primary MSCs and/or mature MSC derived adipocytes grown in 96-well plates were washed with PBS and stained with 100 µl AdipoRed (cat. PT-7009 Lonza, Milan IT), stock diluted 1:40 with PBS, at room temperature for 10 min in the dark. The plate was then analysed using a Genios Pro Plate reader (Tecan) and the fluorescence was quantified (excitation 485 nm; emission 535 nm). Specified drug treatments were included at the concentrations indicated during all stages of cell culture and differentiation during media changes.

2.5. Animals care and use

Female C57BL/6 mice (16–18 g) of 6 weeks of age purchased from Harlan Laboratories (Italy) were dosed with designated treatments by intra-peritoneal injection daily for 5 days and culled on the fifth and final day when the bone marrow was collected. Treatment groups: Vehicle (Kolliphor HS15), CBDA (50 mg·kg^{-1}) and CBG (50 mg·kg^{-1}). The experimental protocol was evaluated and approved by the Institutional Animal Ethics Committee for the use of experimental animals and conformed to guidelines for the safe use and care of experimental animals in accordance with the Italian D.L. no. 116 of 27 January 1992 and associated guidelines in the European Communities Council (86/609/ECC and 2010/63/ UE). Before each experimental procedure, mice were anaesthetized with 75% CO2/25% O2. The experimenter performing behavioural testing was blind for the treatment.

2.6. 2.6 RNA exaction, purification and Real-Time PCR (qPCR)

Total RNA was isolated from MSCs cultured in 6 well-plates. After designated treatments with the compound of interest MSCs were washed in Dulbecco's Phosphate Buffered saline – DPBS $1 \times$ (cat. 14190-094; Gibco, IT) and immersed in 1 ml TRIzol (cat. 15596026; Thermo Fisher Scientific – IT). RNA was subsequently isolated using the Pure link RNA micro Kit (cat. K310010; Thermo Fisher Scientific – IT). Extracted RNA was then treated with DNase-I (1 U/ml; Sigma-Aldrich) fopllowing the manufacturer's instructions. RNA integrity was estimated on a 1% agarose gel. Then, 1 µg of total RNA was reverse transcribed using iScript reverse transcriptase (Biorad, cat. 1708841) following the manufacturer's instructions. Quantitative PCR was performed on independent biological samples ≥ 4 for each experimental group. In addition, each sample was amplified simultaneously in quadruplicate in a one-assay run with a non-template control blank for each primer pair to control for contamination or primer-dimer formation, and the cycle threshold (Ct) value for each experimental group was determined. A housekeeping gene (the ribosomal protein S16) was used to normalize the Ct values, using the $2^{-\Delta Ct}$ formula; differences in mRNA content between groups were expressed as $2^{-\Delta\Delta Ct}$, as previously described [46]. The primer sequences are reported in Table 1.

2.7. MSCs viability

Cell viability was assessed by 3-(4,5-Dimethylthiazol-2-yl)-2,5-diphenyltetrazolium bromide (MTT) assay following published procedures [35]. Briefly, MSCs were seeded at 1×10^4 cells/cm^2 density in 96-well plastic plates. After adhesion, the cells were serum-deprived and treated with the specified concentrations of phytocannabinoids for 24 h and the absence of serum was maintained throughout treatments. After which time the cell media was removed and MTT was added directly to each well, and were incubated for additional 1 h at 37 °C. The absorbance wavelength (OD) of each well was measured at 595 nm on a GENios-Pro 96/384 Multifunction Microplate Reader (GENios-Pro, Tecan, Milan, Italy). Optical density values from control treated cells were defined as 100% of MTT-reducing activity and the treatment effects were measured as a percentage of the inhibition of this control measurement.

2.8. Enzyme-linked immunosorbent assay (ELISA) – adiponectin

The Adiponectin content of cell culture supernatant, collected from MSC derived adipocytes in the presence of designated treatments was quantified using the adiponectin (mouse) ELISA kit (cat. AG-45A-0004YEK-KIO1 AdipoGen Life Sciences). The kit utilizes HRP (HRP conjugated anti-rabbit IgG) and detection (DET) antibody, and the assay was performed according to the manufacturers' instructions. Recombinant mouse adiponectin standard was used to generate the seven-point ELISA standard curve.

2.8.1. Western blotting

BM-MSCs were subjected to western blot analysis following the procedure previously described [47]. Briefly, following the treatment with palmitate and/or phytocannabinoids, differentiated BM-MSCs were homogenized in lysis buffer composed of $1 \times$ TNE, 1% (v/v) Triton X-100, protease (cat. n. P8340, Sigma-Aldrich, MI Italy) and phosphatase (cat. n. P5726, Sigma-Aldrich, MI Italy) inhibitor cocktails at pH 7.4. Lysates were incubated with orbital shaking at 220 rpm at 4 °C for 30 min and then centrifuged for 15 min at 13,000 g at 4 °C. The supernatants were transferred to tubes and quantified by DC Protein Assay (Bio-Rad, Milan, Italy). Subsequently, the samples (60 µg of total protein) were heated at 70 °C for 10 min in Nu-PAGE LDS Sample Buffer (cat. n. NP0007, Life Technologies, Milan, Italy) plus Sample Reducing Agent (cat. n. NP0004, Life Technology Milan, Italy) and loaded on 4–12% Bis-Tris Protein Gels (cat. n. NP0336PK2, Life Technology, Milan, Italy). The gel was run at 165 V for 40 min using MES SDS Running Buffer (cat. B000202, Life Technologies) and then transferred to a PVDF membrane using a Trans-Blot Turbo Transfer System (Bio-Rad, Milan IT). After transfer, the membrane was blocked using 5% dry fat milk (cat. 70166, Sigma Aldrich Milan IT). The primary antibodies used were diluted in Tris-buffered saline (TBS) ($1 \times$) containing 5% milk and 0.1% 0.1% Tween-20 (cat. P1379, Sigma Aldrich Milan IT). The primary antibodies were: a) AKT (9272, Cell Signalling, USA; diluted 1:1000) and b) Phospho-AKT (Ser473) XP (4060, Cell Signalling, USA; diluted 1:2000). The secondary antibody was diluted in the same primary antibody's buffer. We used a Goat Anti-Rabbit IgG (H + L)-HRP Conjugate (cat. 1706515). Reactive bands were detected by chemiluminescence (ECL-plus cat. 1705060; Bio-Rad, Milan, Italy). The intensity of bands was analysed on a ChemiDoc station with Quantity-one software (Biorad, Milan, Italy).

2.8.2. Glucose uptake assay

The glucose uptake in BM-MSCs was measured using the commercially available kit Glucose Uptake-Glo™ Assay (cat. J1341) purchased from Promega (Milan, Italy) following the manufactures' indications. Briefly, BM-MSCs were differentiated in were differentiated in 24-well culture plates. After 12 h of serum deprivation followed by palmitate (± CBD and CBG) treatment for 16 h, the cells were washed 3 times with PBS, and then stimulated with 100 nM insulin at 37 °C for 20 min [48]. The bioluminescent signal was acquired on a Glomax luminometer (Promega, Italy).

2.8.3. Osteocytes (Alizarin Red S)

A 2% Alizarin Red S staining solution was prepared using PBS. The differentiated MSCs were washed in PBS and fixed at room temperature using 4% PFA at 4 °C for 15 min, after which time the cells were washed with dH$_2$O and stained with filtered 2% Alizarin Red S stain solution at room temperature for 5 min. Following this, the cells were washed with dH$_2$0 (x3). The final wash was with dH$_2$O and left on the cells in preparation for analysis and pictures using the Axio Vert.A1 microscope (Zeiss, USA).

2.8.4. Chondrocytes stain (Alcian blue)

A 1% Alcian blue staining solution was prepared in 3% acetic acid. The differentiated MSCs were washed in PBS and then fixed at room

Table 1
List of primers used in qPCR analysis.

GENE	FORWARD Sequence (5′- > 3′)	REVERSE Sequence (5′- > 3′)
SCA1	AGGAGGCAGCAGTTATTGTGG	CGTTGACCTTAGTACCCAGGA
CD106	AATGACCTGTTCCAGCGAGG	TCACAGCCAATAGCAGCACA
CD105	GTCCCAGGAAGTCTACAAGACA	AGGACTCCCCGCTTCTTCAG
CD73	CCTGCACACAAACGACGTG	CTGGTCTCCGGCATCCAAAA
CD29	TGACCCCAATACCAATCTCCC	CCTGAAGTGAACTTGTGGCAG
CD44	AGAAAAATGGCCGCTACAGTATC	TGCATGTTTCAAAACCCTTGC
CD90	TGCTCTCAGTCTTGCAGGTG	TGGATGGAGTTATCCTTGGTGTT
PDGFRα	TATCCTCCCAAACGAGAATGAGA	GTGGTTGTAGTAGCAAGTGTACC
CB1	GGGCACCTTCACGGTTCTG	GTGGAAGTCAACAAAGCTGTAGA
CB2	AGAAAGCCCTCGTACCTGTTC	ATGGTCACACTGCCGATCTTC
PPARγ	GTCGGTTTCAGAAGTGCCTTG	GCTTTGGTCAGCGGGAAG
FABP4	TGTGATGCCTTTGTGGCAACCTG	TATGATGCTCTTCACCTTCCTGTCG
C/EBPA	CAAGAACAGCAACGAGTACCG	GTCACTGGTCAACTCCAGCAC
UCP1	AGGCTTCCAGTACCATTAGGT	CTGAGTGAGGCAAAGCTGATTT
LPL	GGGAGTTTGGCTCCAGAGTTT	TGTGTCTTCAGGGGTCCTTAG
FAS	GGAGGTGGTGATAGCCGGTAT	TGGGTAATCCATAGAGCCCAG
SCD	TGCCGTGGGCGAGGG	ACTCAGAAG CCCAAAGCT
S16	CTGGAGCCTGTTTTGCTTCTG	TGAGATGGACTGTCGGATGG

A

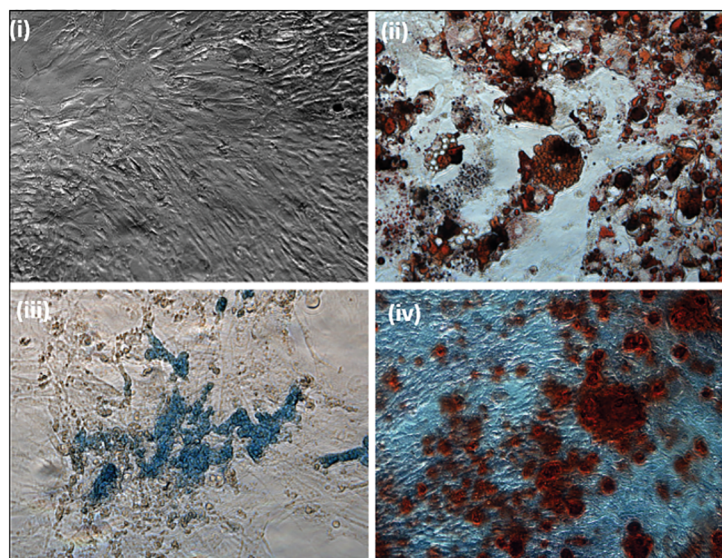| Gene name	MSC (P10)	CHO cells	3T3 cells
SCA-1	19.40 ± 0.22	N.D.	22.98 ± 0.14
CD106	25.69 ± 1.31	N.D.	26.53 ± 0.04
CD105	34.72 ± 1.01	N.D.	34.10 ± 0.45
CD73	29.11 ± 0.70	N.D.	N.D.
CD29	24.76 ± 0.96	19.51 ± 0.03	24.21 ± 0.03
CD44	31.92 ± 0.74	32.39 ± 0.34	35.75 ± 0.55
CD90	25.24 ± 0.98	N.D.	22.68 ± 0.03
PDGFRα	30.65 ± 0.48	N.D.	29.11 ± 0.26
CB1	30.10 ± 0.13	35.74 ± 0.92	32.60 ± 0.19
CB2	31.01 ± 0.26	30.43 ± 0.17	33.54 ± 0.33
S16	18.51 ± 0.27	26.22 ± 0.14	18.55 ± 0.06
GAPDH	18.18 ± 0.06	16.08 ± 0.16	18.52 ± 0.04

B

Fig. 1. Biochemical and phenotypical characterization of isolated BM-MSCs. (A) Table showing the expression degree of specific BM-MSCs markers reported as threshold cycles (Cts) ± Standard Deviation (SD; n = 4). The expression of CB_1 and CB_2 genes is also indicated. CHO and 3T3 cells were used as negative and positive control, respectively. N.D. = signal not detected. Each ct value is the mean of at least four separate determinations. (B) Phase-contrast light transmission images of BM-MSCs cultured in growth media (GM) (i) and differentiated in adipocytes (ii, Oil red), chondrocytes (iii, Alcian blue) and osteocytes (Alzalir Red, S). Obj. 20×. (For interpretation of the references to colour in this figure legend, the reader is referred to the web version of this article.)

temperature using 4% PFA 4 °C for 60 min, after which time the cells were washed with dH_2O and stained with the Alcian blue stain solution at room temperature overnight in the dark. Following this, the cells were washed with dH_2O (x3). The final rinse was with PBS and left on the cells in preparation for analysis and pictures using the Axio Vert.A1 microscope (Zeiss, USA).

2.8.5. Reagents

Rosiglitazone, T0070907, GW7647 and tesaglitazar were purchased from TOCRIS (UK). Kolliphor HS 15 (cat. 42966) and insulin (cat. I6634) were from Sigma-Aldrich (Milan, IT). The phytocannabinoids CBD, CBG, CBDA, CBGA and THCV were provided by GW Research Ltd (UK).

2.8.6. Statistical analysis

Statistical analysis was performed using GraphPad Prism version 8.1.2. The Shapiro-Wilk test was used to determine if a data set was well modelled by a normal distribution or not. Normal data are presented as means ± SEM and non-normal data are presented as box and whisker plots. 'n' refers to the number of samples for each set of experiments. If samples were normally distributed, we used one-way analysis of variance (ANOVA) followed by Tukey's analysis to determine statistically significant differences between two or more independent biological groups. In contrast, for data not normally distributed, we used Kruskal-Wallis test followed by Dunn's test. Outliers were identified by ROUT test. The degrees of freedom 'F (DFn,Dfd) = XXXX; P < 0.XXXX' or H value is indicated in the text as per normal convention. Statistically significant differences were accepted when p was < 0.05.

3. Results

3.1. Phytocannabinoids enhance the capacity of BM-MSCs to generate colony-forming unit-fibroblasts (CFU-F) and differentiate into mature adipocytes.

To isolate BM-MSCs we utilized the colony-forming unit-fibroblast (CFU-F) assay, which selects for the characteristic MSC features of tissue culture plastic-adherence and the ability to self-replicate, thus forming colonies at low cell densities [49]. These isolated colonies of 50 or more fibroblast-like cells were expanded over 3–10 passages to generate a primary cell line of putative BM-MSCs. To assess the effectiveness of our cell isolation procedure at passage 10, we demonstrated clear expression of the positive MSC marker genes CD29, CD44, CD73, CD90, CD105, CD106, PDGFRα and SCA-1, as measured by quantitative PCR (qPCR) (Fig. 1A). Moreover, in agreement with a recent study [22], we found that both CB_1 and CB_2 receptors were expressed in these CFU-F derived cell lines (Fig. 1A). Chinese hamster ovary (CHO) and murine 3 T3 cells were used as a negative and positive control, respectively (Fig. 1A). Furthermore, these cells were induced to differentiate in vitro into chondrogenic, adipogenic and osteogenic cell lineages, demonstrating tri-lineage differentiation ability (Fig. 1B). As such we consider that the cells comprising bone marrow CFU-F colonies display the fundamental characteristics of BM-MSCs.

Therefore, using the CFU-F colony assay, we evaluated the effect of CBD, CBDA, CBG, CBGA and THCV on the number of viable MSC colonies derived from the bone marrow of naive C57BL/6 mice. Our results show that at the concentration of 5 μM CBD, CBDA, CBG and THCV significantly increased the number of BM-MSC colonies (Fig. 2; H = 96,27), with no effects seen at 1 μM, except for CBDA, which showed a numerical increase, but without statistical significance
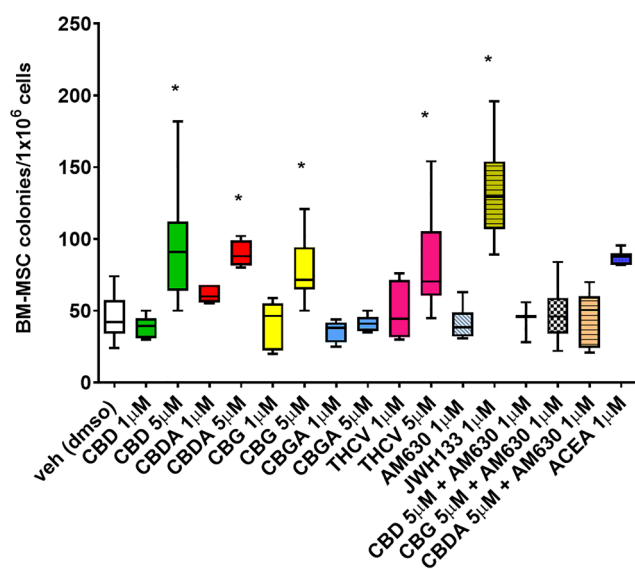

Fig. 2. Effect of CBD, CBG, THCV, CBGA, CBDA, CB_2 selective agonist (JW133) or antagonist (AM630) and CB_1 selective agonist (ACEA) on the number of BM CFU-F colonies ex vivo. Box and whisker plot showing the viability of bone marrow CFU-F colonies after 7 days of in vitro treatment with: vehicle (DMSO < 0.03%; n = 12) in growth media (GM); CBD 1 μM (n = 6); CBD 5 μM (n = 12); CBDA 1 μM (n = 6); CBDA 5 μM (n = 6); CBG 1 μM (n = 6); CBG 5 μM (n = 12); CBGA 1 μM (n = 6); CBGA 5 μM (n = 6); THCV 1 μM (n = 6); THCV 5 μM (n = 12); AM630 1 μM (n = 12); JWH133 1 μM (n = 12); CBD 5 μM plus AM630 (n = 12); CBG 5 μM plus AM630 (n = 12); CBDA 5 μM plus AM630 (n = 12) and ACEA (1 μM; n = 6). The colonies were stained with Giemsa and quantified as described in materials and methods. The Shapiro-Wilk test determined that the data were not normally distributed. Data were compared by use of Kruskal-Wallis test followed by Dunn's test. The asterisk denotes a p value ≤ 0.05 vs vehicle.

(Fig. 2; see Discussion for a description of achievable human plasma concentrations). In contrast, CBGA did not appear to have any effects (Fig. 2). Subsequently, we evaluated whether the effects of these phytocannabinoids were exerted by their interaction with cannabinoid and/or other related classes of receptors. Using JWH133 (1 μM), a selective CB_2 agonist, we observed a robust increase in viable CFU-Fs, while no effect was observed with the selective CB_2 antagonist AM630 (Fig. 2). Of note, the enhanced CFU-F effect of CBD, CBDA, CBG (5 μM) was no longer present when they were co-administered with AM630 (1 μM) (Fig. 2), which indicates a partial contribution of CB_2 receptors to this effect. Most pharmacological antagonists can have off-target effects, and AM630, for example, is known to display activity at TRPA1 [50]. In contrast, the activation of CB_1 receptors by ACEA (1 μM), a selective agonist, only showed a numerical increase, no significant effect (Fig. 2; p value 0.1031). Before selecting the concentrations of phytocannabinoids, we conducted preliminary experiments measuring the viability in BM-MSCs in the presence of increasing concentrations (from 1 to 10 μM) of each phytocannabinoid. The results indicated that none of the phytocannabinoid tested caused significant cytotoxic effects (data not shown).

The pro-adipogenic effect of phytocannabinoids on the capacity of BM-MSCs to differentiate toward mature adipocyte cells as well as their potential interaction with cannabinoid receptors was further explored through the use of lipid droplets fluorescence assay kit. Notably, as shown in Fig. 3, using Nile red (AdipoRed) staining to quantify intracellular triglyceride (TG) levels for the relative analysis of differentiating and fully differentiated mature adipocytes, we found that CBG and CBD significantly promoted the differentiation of BM-MSCs into mature adipocytes, in a concentration-dependent manner. A prominent enhancement of BM-MSCs differentiation was also observed with the combination of CBG 5 μM plus CBD 5 μM (Fig. 4A; H = 155.2). In contrast, CBGA and CBDA did not produce significant effects. Representative light microscope photographs of BM-MSC derived adipocytes differentiated in vitro in the presence or absence of CBG or CBD is shown in Fig. 3. Unexpectedly, the pharmacological stimulation of either CB_1 or CB_2 did not alter the induction of BM-MSC adipocyte differentiation (Fig. 3), and also did not alter CBG and CBD effects (data not shown). For this reason, we hypothesized the involvement of different biological targets for the phytocannabinoids. As mentioned in the introduction, some of phytocannabinoids, including CBGA, CBDA and CBG act as dual PPARα/γ agonists (in a concentration dependent manner, up to 10 μM) with the ability to modulate lipid metabolism [35]. Therefore, to analyse PPAR potential involvement, we first measured the effects of a selective PPARγ agonist (rosiglitazone) or PPARα agonist (GW7647) on BM-MSC adipocyte differentiation. In addition, we also evaluated the effect of tesaglitazar, a potent dual peroxisome PPARα/γ agonist. Our results revealed that the enhancement of induced differentiation in BM-MSCs treated with rosiglitazone was comparable to that observed with CBG and CBD (Fig. 3A). In contrast, the selective stimulation of PPARα using GW7647 was ineffective (Fig. 3A). Of note, the pro-adipogenic effects of CBD and CBG were no longer significant following incubation with T0070907, a selective PPARγ antagonist, which suggests a partial role of this receptor in these effects (Fig. 3A). CBG (5 μM), CBD (5 μM) or rosiglitazone (1 μM) were also tested in undifferentiated MSCs in standard growth media (GM) and all treatments significantly stimulated intracellular TG lipid accumulation; however, under this experimental condition the cells did not generate visible lipid droplets (data not shown). In conclusion, our results indicate that select phytocannabinoids including CBD, CBDA and CBG promote the viability of BM-MSCs in a manner at least in part mediated by CB_2 receptors. However, only CBG and CBD promote BM-MSCs differentiation into mature adipocytes through a mechanism partly dependent on PPARγ receptor activation. THCV did not show significant effects on BM-MSC differentiation (data not shown).
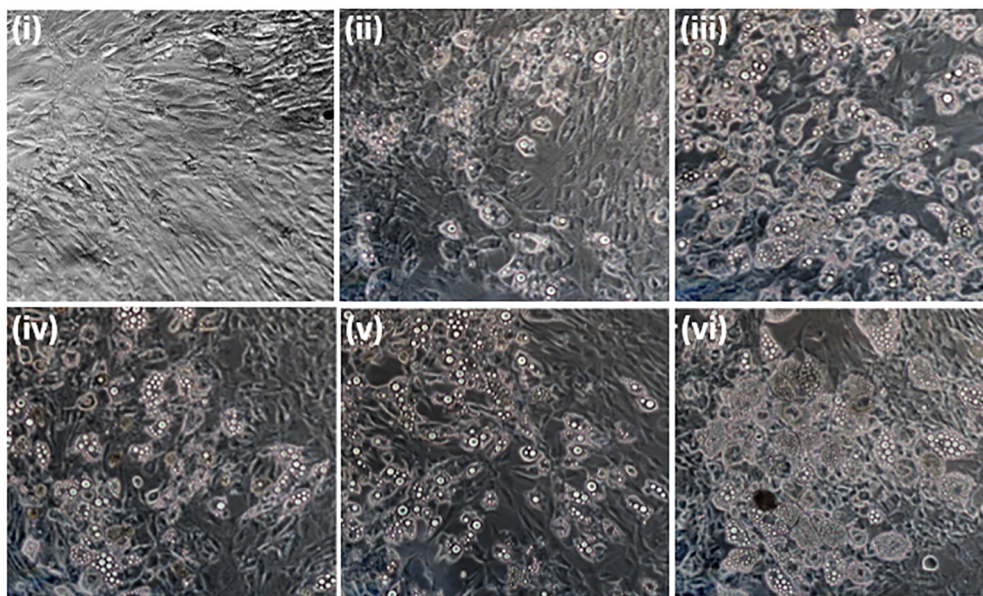
A
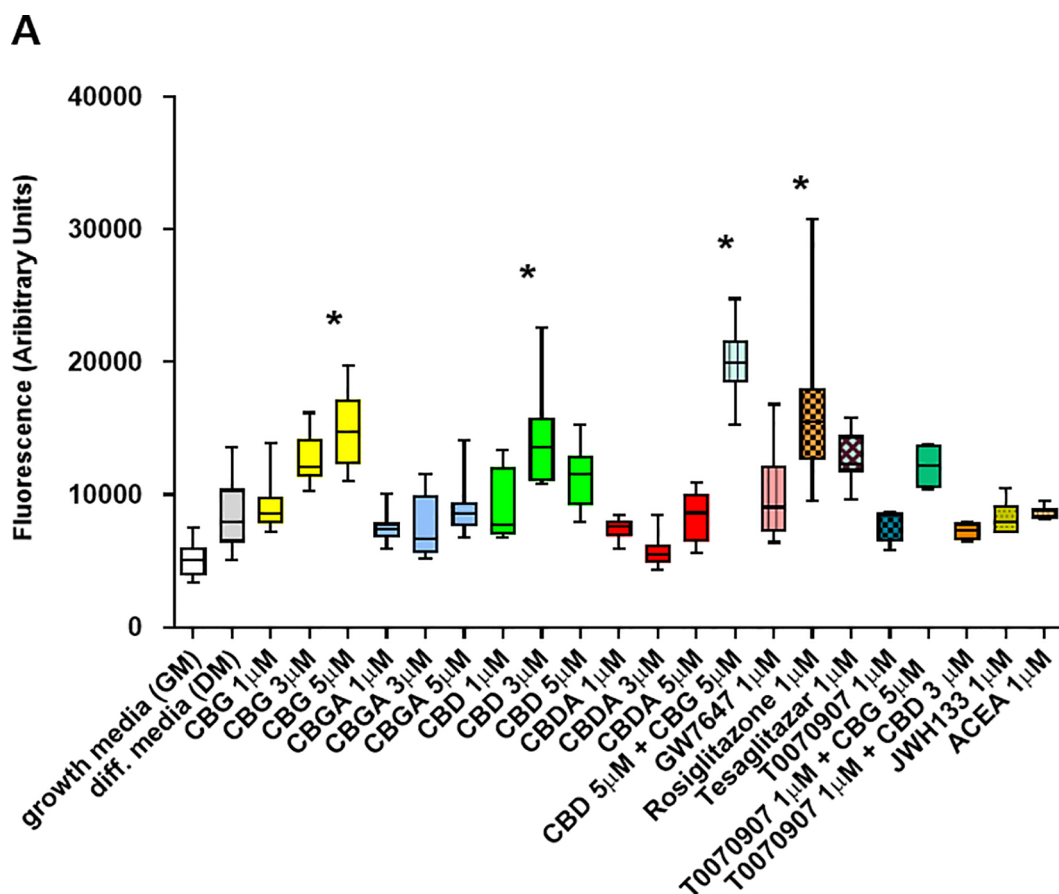
B

Fig. 3. Effect of CBD, CBG, CBGA, CBDA, Rosiglitazone, GW7647, Tesaglitazar, JWH133, T007907 and ACEA in differentiating BM-MSCs. (A) Box and whisker plot showing the effect of vehicle (n = 10); DM (n = 12); CBG 1 µM (n = 10); CBG 3 µM (n = 10); CBG 5 µM (n = 10); CBGA 1 µM (n = 10); CBGA 3 µM (n = 11); CBGA 5 µM (n = 9); CBD 1 µM (n = 10); CBD 3 µM (n = 10); CBD 5 µM (n = 10); CBDA 1 µM (n = 10); CBDA 3 µM (n = 8); CBDA 5 µM (n = 12); GW4757 1 µM (n = 12); Rosiglitazone 1 µM (n = 10); Tesaglitazar 1 µM (n = 10); CBG 5 µM plus T007907 1 µM (n = 4); CBD 5 µM plus T007907 1 µM (n = 4); T007 1 µM (n = 4); JHW133 (n = 6) and ACEA (n = 6) in BM-MSCs induced to differentiate for 14 days. The fluorescent signal reflects the quantity of intracellular lipid droplets as described in materials and methods. The Shapiro-Wilk test determined that the data were not normally distributed. Data were compared by use of Kruskal-Wallis test followed by Dunn's test. The asterisk denotes a p value ≤ 0.05 vs vehicle. (B) Microscope light photographs of MSCs differentiated *ex vitro* for 14 days with designated treatments: (i) standard growth media (GM); (ii) adipocyte differentiation media (DM), (iii) DM + Rosiglitazone (1 µM); (iv) DM + CBD (5 µM); (v) DM + CBG (5 µM) and (vi) DM + CBD plus CBG (5 µM).
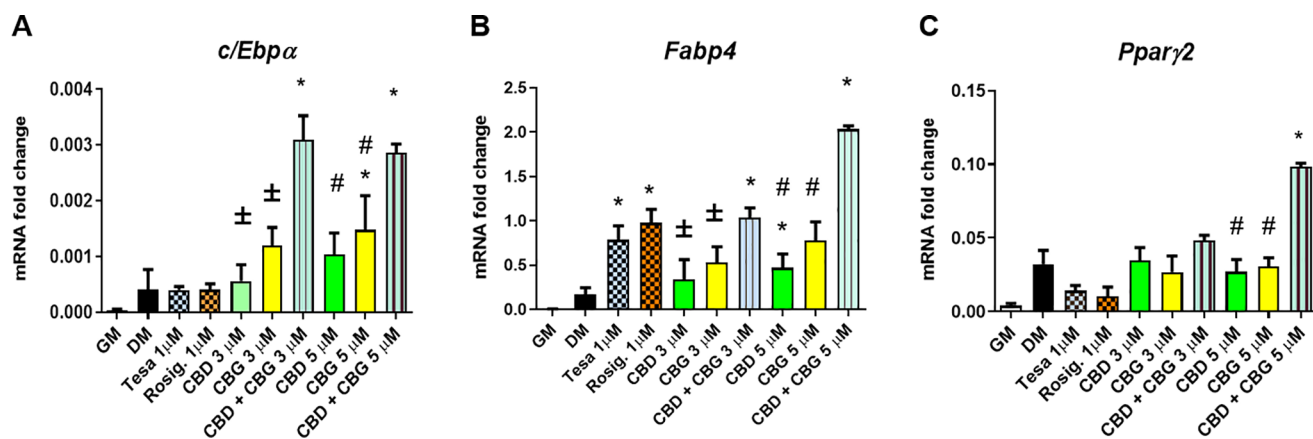
Fig. 4. Effect of CBD, CBG, Rosiglitazone and Tesaglitazar in differentiating BM-MSCs. Bar graphs showing the mRNA expression levels of *c/Ebpα*, *Fabp4*, *PPARγ2* in BM-MSCs exposed to the differentiation media for 14 days ± phytocannabinoids, tesaglitazar or rosiglitazone. The quantification of transcripts was performed by quantitative real-time PCR. Data are expressed as $2^{-\Delta ct}$ formula relative to *S16*, as described in materials and methods. Each bar is the mean ± S.E.M. of three separate determinations. The Shapiro-Wilk test determined that the data were normally distributed. Data sets were compared by use of one-way ANOVA followed by Tukey's test. Differences were considered statistically significant when p was ≤ 0.05. The asterisk denotes a p value ≤ 0.05 vs DM; ± = p ≤ 0.05 vs CBD + CBG (3 μM); # p ≤ 0.05 vs CBD + CBG (5 μM).

3.2. Phytocannabinoid-induced changes in the expression of adipocyte specific regulatory genes

To further understand the observed effects on BM-MSC adipocyte differentiation after 14 days of exposure to adipogenic differentiation media and stimulation with phytocannabinoids, we measured the mRNA expression of the *Pparγ* gene as well as its downstream signalling targets fatty acid binding protein 4 (*Fabp4*) and CCAAT/enhancer binding protein alpha (*C/Ebpα*) [22]. There was no notable alteration in *C/Ebpα* expression in differentiated BM-MSCs at least after 14 days of differentiation [51] (Fig. 4). Likewise, *C/Ebpα* was not altered by tesaglitazar and rosiglitazone compared to control differentiation media (DM) condition. CBG only increased the expression of *C/Ebpα* at 5 μM (F (2, 6) = 9,929; P = 0.0125). Conversely, a different expression profile was observed for *Fabp4*, with CBD 5 μM, tesaglitazar and rosiglitazone all increasing its expression (Fig. 4B). *Pparγ2* expression was not enhanced by CBG, CBD, tesaglitazar or rosiglitazone compared to the control differentiation media (DM) condition. However, combined administration of CBG with CBD resulted in a significantly greater increases in mRNA levels compared to CBD or CBG alone, at the concentration of 3 and 5 μM for *C/Ebpα* and *Fabp4* (Fig. 4A and B; F (9,20) = 31,54; P < 0,0001 for *C/Ebpα*; F (9, 20) = 40.31; P < 0,0001 for *Fabp4*), whereas *Pparγ2* expression was only increased at 5 μM (Fig. 3C; F (9, 20) = 24,76; P < 0,0001).

Next, the expression of additional genes known to play an important regulatory role in orchestrating adipocyte function, including glucose transporter type 4 (*Glut4*), uncoupling protein 1 (*Ucp1*), lipoprotein lipase (*Lpl*), fatty acid synthase (*Fas*), and stearoyl-CoA desaturase (*Scd*) were also evaluated. As evidence of functional adipocyte differentiation, it was confirmed that stimulation of adipogenesis by 1 μM rosiglitazone up-regulated the expression of *Glut4*, the primary insulin-sensitive glucose transporter, 7-fold above the baseline levels of standard MSC adipocyte differentiation (Fig. 5A) and *Glut4* also increased when CBG and CBD were given individually. Notably, CBG and CBD 5 μM treatment in combination produced an increase of *Glut4* expression to an extent numerically greater than Rosiglitazone, even though this difference did not reach statistical significance (Fig. 5A). In addition, we identified low basal expression of *Ucp1* in standard control cells, which was enhanced by CBD (5 μM; when given alone or in combination with CBG) (Fig. 5B), thus inducing a brown or beige-like phenotype. However, CBG and CBD (5 μM) individually did not significantly increase *Ucp1* expression (Fig. 5A; H = 17,64). Similar to the observation for *Glut4*, we found that the combination of CBD plus CBG

produced the most robust increase in the expression levels of *Scd* (H = 14,94), *Fas* (H = 12,86) and *Lpl* (H = 13,54) genes (Fig. 5C–E).

To gain further insight into the effects of phytocannabinoids on BM-MSC adipocyte differentiation, we measured (by ELISA) the secretion of the adipokine, adiponectin, into the cell culture supernatant from MSC derived adipocytes differentiated in the presence of rosiglitazone (1 μM), CBG (5 μM) in combination or not with CBD (5 μM) (Fig. 5B). The level of adiponectin expression in the cell media of control adipocytes on day 14 of differentiation was relatively low compared to the treatment groups tested, but was significantly elevated in adipocytes differentiated in the presence of rosiglitazone (1 μM) and CBG (5 μM) which increased the levels ~18-fold (4.5 vs 0.25 ng/ml), comparable to the effect seen with rosiglitazone (1 μM) (Fig. 6C; H = 14,84). Intriguingly, the combination of CBD + CBG did not further increase the release of adiponectin, compared to the group of cells treated with CBG alone (Fig. 5B).

3.3. Effect of CBD and CBG on palmitate-induced insulin resistance in BM-MSCs

To gain novel insights into the use of phytocannabinoids to treat metabolic disorders associated with adipose tissue dysfunction, we next explored whether the insulin signalling impairment induced by palmitate in BM-MSCs derived adipocytes could be affected by CBD and CBG. There is evidence that the activity of the intracellular kinase AKT is crucial to trigger intracellular signal transduction pathways leading to insulin-mediated glucose uptake [48,52]. Palmitate is known to inhibit AKT phosphorylation (hence activation) and consequently cause insulin resistance, as revealed in numerous experimental models [52–55]. In this study, BM-MSCs were first induced to differentiate in standard DM for 14 days, and subsequently sodium palmitate (NaP; 350 μM) was added to each cell plate in the presence or absence of CBD and CBG and incubated for 18 h [56]. After this time, the cells were stimulated with insulin (100 nM) for 20 min. As shown in Fig. 6A, we found that in differentiated BM-MSCs cells, palmitate significantly reduced AKT phosphorylation. However, in the presence of CBG (alone or in combination CBD) the phosphorylation of AKT was fully recovered. Along with this, we measured glucose uptake under the same experimental conditions. As shown in Fig. 6B, palmitate significantly inhibited insulin-stimulated uptake of glucose. This latter effect was no longer present in cells treated with CBD and CBG.
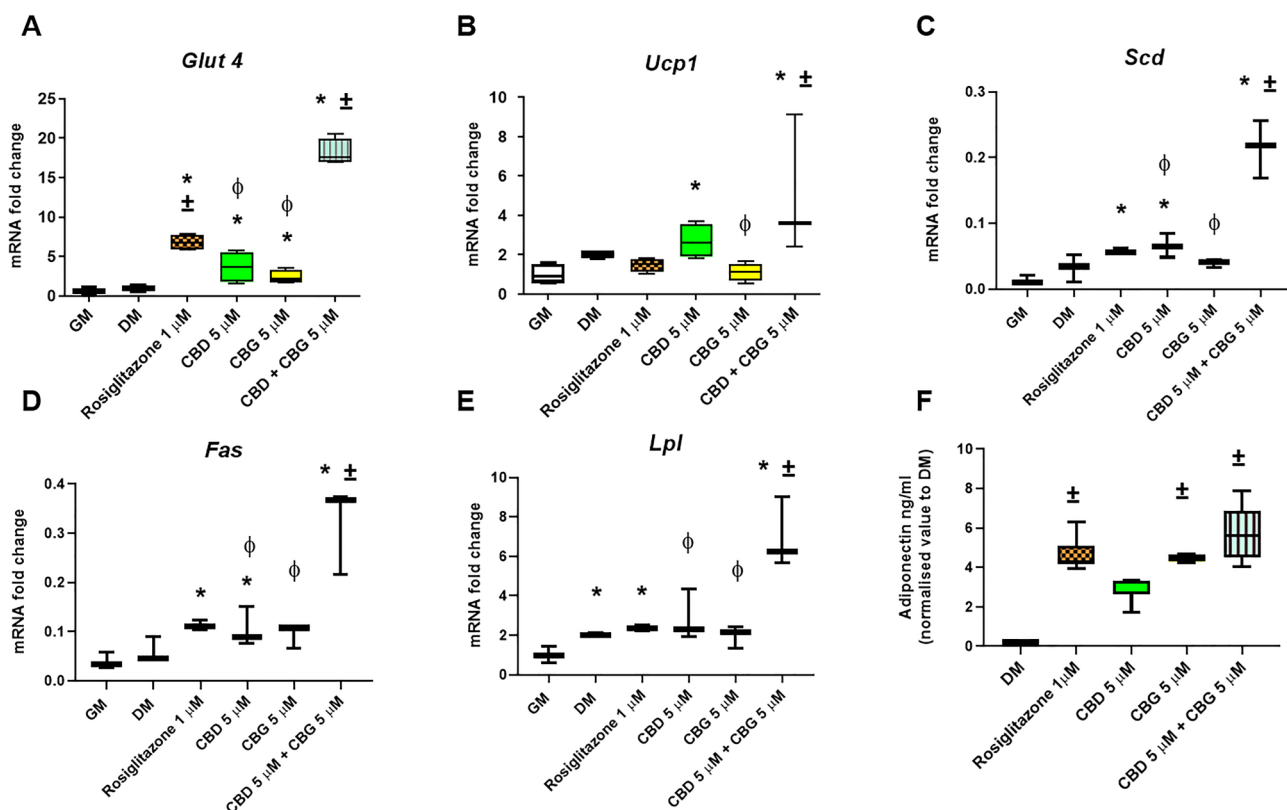
Fig. 5. Effect of CBD and CBG on the expression of adipocytes regulatory genes. (A) Box and whisker plot showing the mRNA expression levels of *Glut4* (A), *Ucp1* (B), *Lpl* (C), *Fas* (D) *and Scd* (E) in BM-MSCs cultured in growth media (GM) or induced to differentiate in differentiation media (DM) for 14 days ± phytocannabinoids or Rosiglitazone. The quantification of transcripts was performed by quantitative real-time PCR. (F) Levels of adiponectin in BM-MSCs derived adipocyte culture supernatant induced to differentiate for 14 days in presence of vehicle (DMSO 0.003%; n = 3), rosiglitazone (1 μM; n = 6), CBD (5 μM; n = 6), CBG (5 μM; n = 4) and CBD + CBG (5 μM; n = 4) as quantified by ELISA. The Shapiro-Wilk test determined that the data were not normally distributed. Data were compared by use of Kruskal-Wallis test followed by Dunn's test. The asterisk denotes a *p* value ≤ 0.05 vs GM; ± = p ≤ 0.05 vs DM; The symbol φ denotes a *p* value ≤ 0.05 vs CBD + CBG 5 (μM).

3.4. Phytocannabinoids enhance the number of BM-MSC colony forming unit-fibroblasts (CFU-Fs) that comprise adipocyte progenitors in vivo

As demonstrated above, among all the phytocannabinoids tested, CBDA, CBG, CBD and THCV at 5 μM all promoted the formation of CFU-F colonies *in vitro* (Fig. 2). In light of this evidence, we extended our

study to evaluate whether these effects were retained *in vivo*, specifically selecting CBG and CBDA. To this purpose, C57BL/6 mice were intraperitoneally injected daily with vehicle, CBG (50 mg/kg), CBDA (50 mg/kg) or a combination of CBG (50 mg/kg) and CBDA (50 mg/kg) for 5 days, after which bone marrow CFU-Fs were generated. As compared to the data obtained *in vitro*, we found that CBDA, but not CBG,
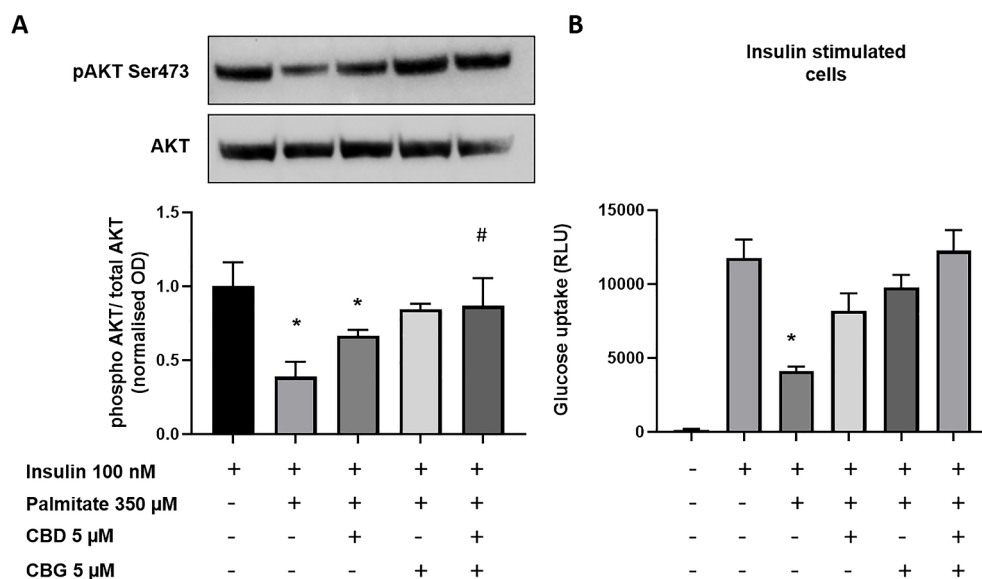

Fig. 6. Effect of CBD and CBG on palmitate-induced insulin resistance induced in differentiated BM-MSCs. (A) *Upper part* Representative blot showing the band intensity of phospho (ser473) and total AKT in differentiated BM-MSCs treated with sodium palmitate 350 μM for 18 h. *Lower part* Bar graphs showing the quantification of phospho AKT levels normalized to total AKT. Data represent the means ± S.E.M. of three separate determinations. (B) Levels of glucose uptake expressed as relative luminescence units (RLU) in insulin-stimulated BM-MSCs. The Shapiro Wilk test determined that the data were normally distributed. Data sets were compared by one-way ANOVA followed by Tukey's test. Differences were considered statistically significant when p was ≤ 0.05. The asterisk (*) denotes a p value of ≤ 0.05 vs the vehicle control group; the hash (#) denotes a p value of ≤ 0.05 vs the palmitate treated group.
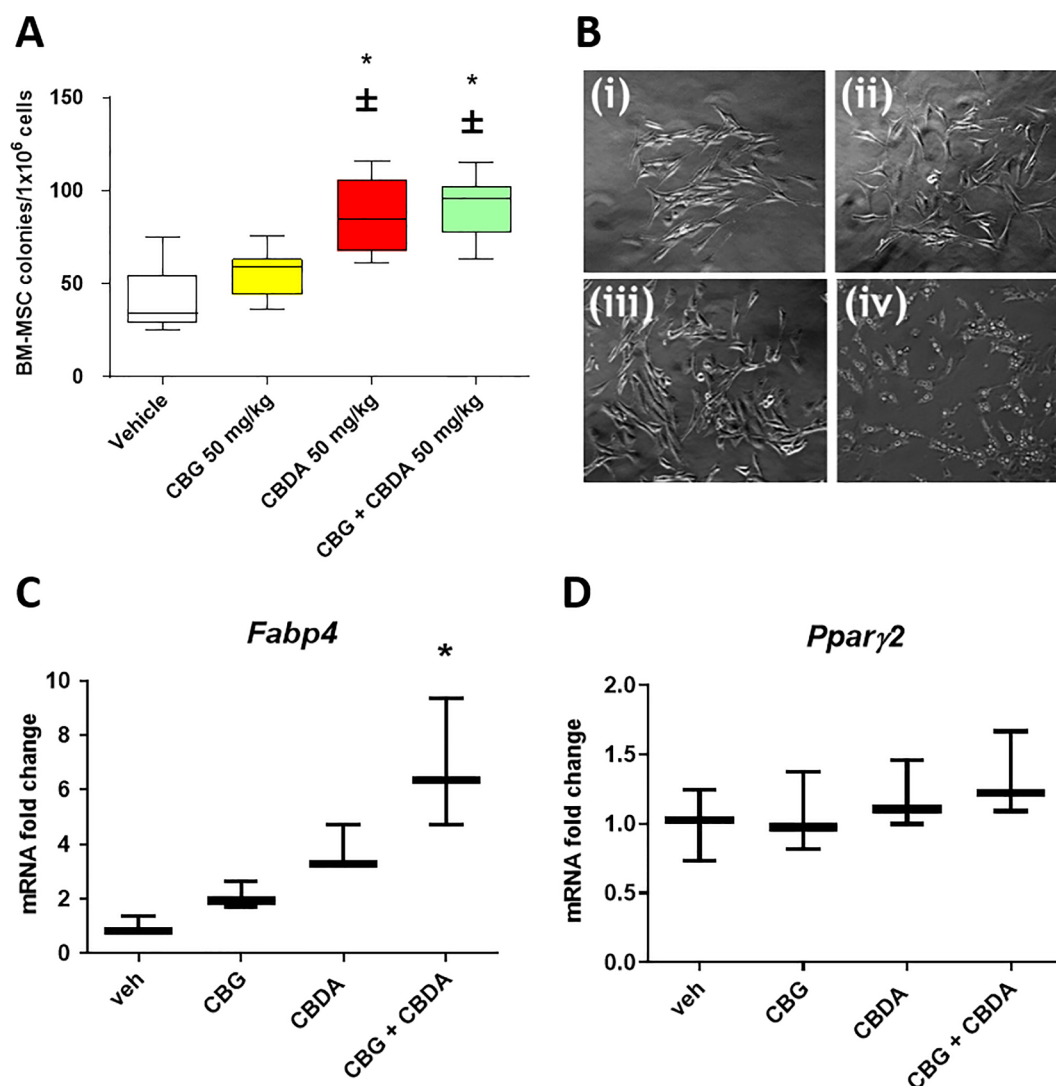
Fig. 7. Effect of CBDA and CBG on the number of BM CFU-F colonies *in vivo*. (A) The number of bone marrow CFU-F colonies after 5 days of consecutive *in vivo* treatment with CBG (50 mg/kg), CBDA (50 mg/kg) or their combination. (B) Microscope light photographs of MSCs differentiated *ex vitro* for 14 days with: (i) standard growth media (GM); (ii) CBG (50 mg/kg), (iii) CBDA (50 mg/kg); (iv) CBD + CBG (50 mg/kg). The quantification of *Fabp4* (C) and *Pparγ2* (D) transcript levels were performed by quantitative real-time PCR. Box and whisker plots of at least four separate determinations. The Shapiro-Wilk test determined that the data were not normally distributed. Data were compared by use of Kruskal-Wallis test followed by Dunn's test. The asterisk denotes a *p* value ≤ 0.05 vs vehicle; ± = p ≤ 0.05 vs CBG.

significantly enhanced the number of CFU-Fs (Fig. 7A and B; H value = 23.35). The combination of CBDA and CBG also resulted in a significant elevation in CFU-F colonies, but there did not appear to be any additive effects. (Fig. 7A and B). Furthermore, qPCR was used to assess the adipogenic differentiation potential of the CFU-Fs colonies generated, demonstrating that *in vivo* treatment with a combination of CBG (50 mg/kg) and CBDA (50 mg/kg) enhanced the incidence of CFU-Fs with a pre-determined adipocyte precursor phenotype after 14 days (Fig. 7C), as demonstrated by the up-regulation of *Fabp4* in standard cell culture media, an effect that was absent when CBG (50 mg/kg) and CBDA (50 mg/kg) were administered individually. *Pparγ2* expression within the CFU-Fs was not significantly altered by any of the *in vivo* treatment groups (Fig. 7D).

4. Discussion

The ECS regulates adipose tissue metabolism [57], and endocannabinoid tone in adipocytes is maintained by feedback from hormones, transcription factors, adipokines, and insulin [58]. These are often altered during metabolic disorders, causing ECS deregulation that exacerbates these pathologies [58,59]. Adipogenesis requires clonal expansion of MSCs followed by terminal differentiation; thus, MSCs represent a target for therapeutic intervention to regenerate functional adipose tissue and reestablish energy metabolism homeostasis. However, the safety and heterogeneity of exogenous MSCs administered clinically is currently under evaluation [60].

There is evidence that the ECS regulates stem cell fate decisions (*i.e.* survival, proliferation, differentiation and cell-cycle dynamics), determining the formation of organs and tissues including adipose [57,61,62]. In this study, we demonstrated that some non-euphoric compounds present in *Cannabis sativa* enhance the number of viable undifferentiated bone marrow CFU-Fs *in vitro*, with CBDA, CBG, CBD and THCV all showing efficacy at 5 μM. These results are in agreement with the work of Scutt A et al. 2007, who showed an enhancement of osteogenic bone marrow CFU-Fs after various phytocannabinoid including cannabidivarin (CBDV), cannabigerol (CBG), cannabinol (CBN), cannabidiol (CBD), THC, and tetrahydrocannabivarin (THCV), all at 10 μM [40]. Notably, we present evidence that the selected phytocannabinoids may exert their effects at least in part through CB_2 receptors, since their effects are no longer statistically significant in the

presence of a specific CB_2 antagonist, *i.e.* AM630. Currently, the achievable safe concentrations of these phytocannabinoids in bone marrow is unknown. However, it should be noted that the 5 μM concentration of phytocannabinoids is in excess of plasma concentrations achieved in the clinic; healthy volunteers who received botanically derived purified CBD oral solution ~21.4 mg/kg/day for six days achieved a plasma C_{max} of 330.3 ng/mL, which equates to 1.04 μM. Using primary MSCs expanded from bone marrow CFU-Fs, a physiologically relevant adipocyte progenitor model to recapitulate differentiating adipocytes, we also quantified, for the first time, the positive effect of the phytocannabinoids on adipogenic induction and this effect was not mediated by CB_2.

CBG, CBGA, CBD and CBDA all have partial *PPARγ* agonist activity in the low μM range (up to 10 μM), and CBG, CBGA and CBDA (up to 10 μM) are also partial *PPARα* agonists [35,63]. *PPARγ* receptors play a pivotal role in adipogenesis; hence potent *PPARγ* agonists have been used clinically to treat metabolic disorders including T2DM, reducing hyperglycemia, hyperinsulinemia and hyperlipidemia [64,65]. *PPARα* stimulation, by comparison, maintains adipocyte lipid profile arrays, improving dyslipidemia by regulating lipogenesis and beta-oxidation (59), while raising the levels of high-density lipoprotein cholesterol (HDL-C) [66]. Consequently, dual PPARα/γ agonists are thought to enhance therapeutic potential, simultaneously regulating hyperglycemic and dyslipidaemic systems [67]. Here, we demonstrated that adipocyte differentiation of MSCs induced *in vitro*, as quantified by changes in intracellular TG accumulation, is significantly enhanced in dose dependent manners by either CBG or CBD, and this effect is absent in the presence of a selective PPARγ antagonist T0070907. The pharmacodynamics of CBG and/or CBD on MSC adipogenesis was further characterized by individual dose response treatments, revealing a similar adipocyte gene induction efficacy, since they enhanced the expression of the mature adipocyte markers *C/Ebpα*, *Fabp4*, *Fas* and *Scd* [68], supporting the premise that their effect involves signaling via PPARγ activation [69].

Previous research demonstrated that CBD, as monotherapy or in combination with other phytocannabinoids, shows neuroprotective properties [35]. Accordingly, CBG in combination with CBD was found here to be additive, by improving the overall efficacy in adipocyte gene induction assays as compared to individual treatments, specifically *Pparγ2*, *Fabp4*, *C/Ebpα*, *Lpl*, *Fas*, *Glut4 and Scd* expression. This observation was also substantiated functionally by the finding of significantly enhanced lipid accumulation in the differentiation of adipocytes after treatment with a combination of these two phytocannabinoids.

Following on from the *in vitro* data, CBDA and CBG were tested *in vivo*, since CBDA produced a robust effect on CFU-F numbers, whereas CBG exerted a strong pro-adipogenic effect. Encouragingly, the *in vivo* data was consistent with the *in vitro* observations and the endogenous bone marrow CFU-Fs were increased after administration of CBDA, and its combination with CBG showed no enhanced effect. Contrary to the pro-adipogenic effect of CBG, CBDA did not alter the differentiation to adipocytes of primary MSCs *in vitro*. However, CBDA promoted a higher proportion of *Fabp4* positive adipocyte progenitors within these BM-MSC colonies. Some colonies underwent sporadic autonomous adipocyte differentiation, with visible lipid droplets (Fig. 7B), indicating a cell lineage selection bias for stromal populations of committed adipocyte progenitors primed for induction of adipogenesis [70]. This corroborates previous research where combination treatments with acidic cannabinoids, such as CBDA, improved the potency of other phytocannabinoids [71,72].

Adipose tissue insulin resistance is characterized by a deficiency in GLUT4 [73], thus effective adipogenesis must re-establish insulin sensitivity to maintain normoglycaemia. Rosiglitazone is a well-established insulin-sensitizer and acts in part by enhancing GLUT4 expression [74]. In our *in vitro* experiments, CBG and CBD, when given alone or in combination, prevented the palmitate-induced insulin sensitivity impairment in differentiating BM-MSCs by increasing *Glut4* mRNA expression (Fig. 4A) as well as by fully recovering AKT activation and glucose uptake (Fig. 6). This suggests that CBD and CBG might be an effective treatment for insulin sensitization, at least at a concentration of 5 μM and under conditions leading to increased BM-MSC differentiation into adipocytes. In addition, combined treatment with CBG and CBD formed multilocular adipocytes [75] and elevated the expression of *Ucp1*, a marker of beige and brown adipose tissue (BAT), suggesting that these phytocannabinoids could enhance fatty acid oxidation and thermogenesis [76]. The terminal stages of BAT differentiation are induced by PPARα [77,78], and therefore this effect might also be due to the PPARα agonist activity of CBG [35]. Obesity inhibits BAT formation, negatively impacting on systemic lipid metabolism [79], and our data suggests that these phytocannabinoid treatments may potentially alleviate this pathology.

Adiponectin is an important regulator of glucose and fatty acid oxidation that is inversely correlated with obesity [80]. Systemic adiponectin is controlled by BM-MSC derived adipocytes [81], which in turn maintains the BM-MSC stem cell niche [82]. Here we show that rosiglitazone treatment during adipogenesis enhanced adiponectin levels secreted from the resulting adipocytes in agreement with existing data [83] and this same response was also seen after CBG treatment, indicative that CBG represents an alternative candidate to enhance adipose endocrine function.

Adipose tissue can regulate energy homeostasis [58], and accordingly MSC dysfunction, senescence and depletion is prevalent in metabolic syndromes [84], dysregulating adipogenesis and adipose tissue function. Consequently, this results in compensatory adipocyte hypertrophy, which stimulates lipolysis, ectopic fat and excessive adipose tissue, promoting systemic inflammation and insulin resistance [85]. Thus, a relevant treatment strategy could be to augment endogenous BM-MSCs to stimulate optimal adipogenesis to reinstate functional insulin sensitive juvenile adipocytes, temporarily restoring metabolic energy homeostasis and reducing permanent damage to pancreatic β-cells (for example) [86]. Accordingly, thiazolidinediones (TZD) are potent specific PPARα/γ agonists and act as adipogenesis stimulators and insulin sensitizers, and were previously used clinically for the treatment of T2DM [87], although unfortunately their use was associated with adverse side effects and has been restricted or banned [88]. The results presented in this paper suggest that select non-euphoric phytocannabinoids, *i.e.* CBDA, CBG or CBD, either individually or in combination, modulate multiple relevant receptors, including CB_2 (possibly indirectly, since these compounds do not possess agonist activity at CB_2 at the concentrations used in this study, so further investigations are required) and PPARγ, whose simultaneous activation appear to demonstrate additivity, promoting the targeted enhancement of viable endogenous BM-MSCs and their adipogenic potential, respectively. This may bypass the problems associated with exogenous MSC delivery [89] by actively directing MSC lineage fate to transition into committed adipocyte progenitors and the subsequent enhancement of adipogenic induction capacity, selecting for specific functional mature adipocyte subtypes, *e.g.* white, beige or brown adipocytes.

The promiscuous pharmacology of phytocannabinoids makes them viable candidates for new medicines for the treatment of metabolic syndromes through the simultaneous resolution of collective complications due to impaired development, maintenance, activity and function of the adipose tissue. Furthermore, phytocannabinoids are generally well tolerated in comparison to potent synthetic PPAR agonists, and combination treatments may further improve their efficacy at lower doses [88]. Future studies should be carried out using clinically meaningful doses in clinically relevant animal models of pathologies originating from adipocyte dysfunction, *e.g.* T2DM or lipodystrophy [45] where these compounds may allow for the restoration of adipose tissue function and the reinstatement of insulin sensitivity, which provide a requisite metabolic safe haven to sequester excess energy or promote energy expenditure via thermogenesis, with the aim to

regulate energy homeostasis by reducing blood glucose, blood lipids and ectopic lipid accumulation.

CRediT authorship contribution statement

Tariq Fellous: Conceptualization, Methodology, Investigation, Data curation, Writing - original draft, Writing - review & editing. **Fabrizia De Maio:** Conceptualization, Methodology, Investigation. **Hilal Kalkan:** Methodology, Investigation. **Biagio Carannante:** Methodology, Investigation. **Serena Boccella:** Methodology, Investigation. **Stefania Petrosino:** Methodology, Investigation. **Sabatino Maione:** Conceptualization, Methodology, Investigation. **Vincenzo Di Marzo:** Conceptualization, Data curation, Writing - original draft, Writing - review & editing. **Fabio Arturo Iannotti:** Methodology, Investigation, Data curation, Writing - original draft, Writing - review & editing.

Acknowledgments

Declaration of Competing Interest

F.A.I. and V.D. are recipient of research grants from GW Research Ltd, Cambridge, UK. V.D. is a consultant with GW Research Ltd.

References

[1] A.V.B. Castro, C.M. Kolka, S.P. Kim, R.N. Bergman, Obesity, insulin resistance and comorbidities – mechanisms of association, Arq. Bras. Endocrinol. Metabol. 58 (2014) 600–609.

[2] S. Bobis, D. Jarocha, M. Majka, Mesenchymal stem cells: characteristics and clinical applications, Folia Histochem. Cytobiol. 44 (2006) 215–230.

[3] S. Gronthos, D.M. Franklin, H.A. Leddy, P.G. Robey, R.W. Storms, J.M. Gimble, Surface protein characterization of human adipose tissue-derived stromal cells, J. Cell. Physiol. 189 (2001) 54–63, https://doi.org/10.1002/jcp.1138.

[4] N.J. Zvaifler, L. Marinova-Mutafchieva, G. Adams, C.J. Edwards, J. Moss, J.A. Burger, R.N. Maini, Mesenchymal precursor cells in the blood of normal individuals, Arthritis Res. 2 (2000) 477–488, https://doi.org/10.1186/ar130.

[5] C. Campagnoli, I.A. Roberts, S. Kumar, P.R. Bennett, I. Bellantuono, N.M. Fisk, Identification of mesenchymal stem/progenitor cells in human first-trimester fetal blood, liver, and bone marrow, Blood 98 (2001) 2396–2402.

[6] P.S. in 't Anker, W.A. Noort, S.A. Scherjon, C. Kleijburg-van der Keur, A.B. Kruisselbrink, R.L. van Bezooijen, W. Beekhuizen, R. Willemze, H.H.H. Kanhai, W.E. Fibbe, Mesenchymal stem cells in human second-trimester bone marrow, liver, lung, and spleen exhibit a similar immunophenotype but a heterogeneous multi-lineage differentiation potential, Haematologica 88 (2003) 845–852.

[7] R. Hass, C. Kasper, S. Böhm, R. Jacobs, Different populations and sources of human mesenchymal stem cells (MSC): a comparison of adult and neonatal tissue-derived MSC, Cell Commun. Signal. 9 (2011) 12, https://doi.org/10.1186/1478-811X-9-12.

[8] M. Rydén, M. Uzunel, J.L. Hård, E. Borgström, J.E. Mold, E. Arner, N. Mejhert, D.P. Andersson, Y. Widlund, M. Hassan, C.V. Jones, K.L. Spalding, B.-M. Svahn, A. Ahmadian, J. Frisén, S. Bernard, J. Mattsson, P. Arner, Transplanted bone marrow-derived cells contribute to human adipogenesis, Cell Metab. 22 (2015) 408–417, https://doi.org/10.1016/j.cmet.2015.06.011.

[9] K. Matsushita, Mesenchymal stem cells and metabolic syndrome: current understanding and potential clinical implications, Stem Cells Int. 2016 (2016) 2892840, https://doi.org/10.1155/2016/2892840.

[10] K. Matsushita, V.J. Dzau, Mesenchymal stem cells in obesity: insights for translational applications, Lab. Invest. J. Tech. Methods Pathol. 97 (2017) 1158–1166, https://doi.org/10.1038/labinvest.2017.42.

[11] J. Kang, L. Zhang, X. Luo, X. Ma, G. Wang, Y. Yang, Y. Yan, H. Qian, X. Zhang, W. Xu, F. Mao, Systematic exposition of mesenchymal stem cell for inflammatory bowel disease and its associated colorectal cancer, BioMed. Res. Int. 2018 (2018) 9652817, https://doi.org/10.1155/2018/9652817.

[12] F. Rad, M. Ghorbani, A. Mohammadi Roushandeh, M. Habibi Roudkenar, Mesenchymal stem cell-based therapy for autoimmune diseases: emerging roles of extracellular vesicles, Mol. Biol. Rep. (2019), https://doi.org/10.1007/s11033-019-04588-y.

[13] A. Kakkar, A. Sorout, M. Tiwari, P. Shrivastava, P. Meena, S.K. Saraswat, S. Srivastava, R. Datt, S. Pandey, Current status of stem cell treatment for type I diabetes mellitus, Tissue Eng. Regen. Med. 15 (2018) 699–709, https://doi.org/10.1007/s13770-018-0143-9.

[14] P. Marrazzo, A.N. Crupi, F. Alviano, L. Teodori, L. Bonsi, Exploring the roles of

[15] H. Vilaça-Faria, A.J. Salgado, F.G. Teixeira, Mesenchymal stem cells-derived exosomes: a new possible therapeutic strategy for Parkinson's disease? Cells 8 (2019), https://doi.org/10.3390/cells8020118.

[16] V. Turinetto, E. Vitale, C. Giachino, Senescence in human mesenchymal stem cells: functional changes and implications in stem cell-based therapy, Int. J. Mol. Sci. 17 (2016), https://doi.org/10.3390/ijms17071164.

[17] F.A. Iannotti, V. Di Marzo, S. Petrosino, Endocannabinoids and endocannabinoid-related mediators: targets, metabolism and role in neurological disorders, Prog. Lipid Res. 62 (2016) 107–128, https://doi.org/10.1016/j.plipres.2016.02.002.

[18] L. Cristino, T. Bisogno, V. Di Marzo, Cannabinoids and the expanded endocannabinoid system in neurological disorders, Nat. Rev. Neurol. (2019), https://doi.org/10.1038/s41582-019-0284-z.

[19] L.M. Krott, F. Piscitelli, M. Heine, S. Borrino, L. Scheja, C. Silvestri, J. Heeren, V. Di Marzo, Endocannabinoid regulation in white and brown adipose tissue following thermogenic activation, J. Lipid Res. 57 (2016) 464–473, https://doi.org/10.1194/jlr.M065227.

[20] C. Pagano, C. Pilon, A. Calcagno, R. Urbanet, M. Rossato, G. Milan, K. Bianchi, R. Rizzuto, P. Bernante, R. Federspil, R. Vettor, The endogenous cannabinoid system stimulates glucose uptake in human fat cells via phosphatidylinositol 3-kinase and calcium-dependent mechanisms, J. Clin. Endocrinol. Metab. 92 (2007) 4810–4819, https://doi.org/10.1210/jc.2007-0768.

[21] I. Matias, M.-P. Gonthier, P. Orlando, V. Martiadis, L. De Petrocellis, C. Cervino, S. Petrosino, L. Hoareau, F. Festy, R. Pasquali, R. Roche, M. Maj, U. Pagotto, P. Monteleone, V. Di Marzo, Regulation, function, and dysregulation of endocannabinoids in models of adipose and beta-pancreatic cells and in obesity and hyperglycemia, J. Clin. Endocrinol. Metab. 91 (2006) 3171–3180, https://doi.org/10.1210/jc.2005-2679.

[22] S.E. O'Sullivan, An update on PPAR activation by cannabinoids, Br. J. Pharmacol. 173 (2016) 1899–1910, https://doi.org/10.1111/bph.13497.

[23] K. Rohrbach, M.A. Thomas, S. Glick, E.N. Fung, V. Wang, L. Watson, P. Gregory, J. Antel, M.A. Pelleymounter, Ibipinabant attenuates β-cell loss in male Zucker diabetic fatty rats independently of its effects on body weight, Diabetes Obes. Metab. 14 (2012) 555–564, https://doi.org/10.1111/j.1463-1326.2012.01563.x.

[24] T. Jourdan, G. Godlewski, R. Cinar, A. Bertola, G. Szanda, J. Liu, J. Tam, T. Han, B. Mukhopadhyay, M.C. Skarulis, C. Ju, M. Aouadi, M.P. Czech, G. Kunos, Activation of the Nlrp3 inflammasome in infiltrating macrophages by endocannabinoids mediates beta cell loss in type 2 diabetes, Nat. Med. 19 (2013) 1132–1140, https://doi.org/10.1038/nm.3265.

[25] V. Deveaux, T. Cadoudal, Y. Ichigotani, F. Teixeira-Clerc, A. Louvet, S. Manin, J.T.-V. Nhieu, M.P. Belot, A. Zimmer, P. Even, P.D. Cani, C. Knauf, R. Burcelin, A. Bertola, Y. Le Marchand-Brustel, P. Gual, A. Mallat, S. Lotersztajn, Cannabinoid CB2 receptor potentiates obesity-associated inflammation, insulin resistance and hepatic steatosis, PLoS One 4 (2009) e5844, , https://doi.org/10.1371/journal.pone.0005844.

[26] G. Gruden, F. Barutta, G. Kunos, P. Pacher, Role of the endocannabinoid system in diabetes and diabetic complications, Br. J. Pharmacol. 173 (2016) 1116–1127, https://doi.org/10.1111/bph.13226.

[27] F. Rossi, M.E. Bernardo, G. Bellini, L. Luongo, A. Conforti, I. Manzo, F. Guida, L. Cristino, R. Imperatore, S. Petrosino, B. Nobili, V. Di Marzo, F. Locatelli, S. Maione, The cannabinoid receptor type 2 as mediator of mesenchymal stromal cell immunosuppressive properties, PLoS One 8 (2013) e80022, , https://doi.org/10.1371/journal.pone.0080022.

[28] A. Gowran, K. McKayed, V.A. Campbell, The cannabinoid receptor type 1 is essential for mesenchymal stem cell survival and differentiation: implications for bone health, Stem Cells Int. 2013 (2013) 796715, , https://doi.org/10.1155/2013/796715.

[29] Y.-X. Sun, A.-H. Xu, Y. Yang, J.-X. Zhang, A.-W. Yu, Activation of cannabinoid receptor 2 enhances osteogenic differentiation of bone marrow derived mesenchymal stem cells, BioMed. Res. Int. 2015 (2015) 874982, , https://doi.org/10.1155/2015/874982.

[30] L. Wang, L. Yang, L. Tian, P. Mai, S. Jia, L. Yang, L. Li, Cannabinoid receptor 1 mediates homing of bone marrow-derived mesenchymal stem cells triggered by chronic liver injury, J. Cell. Physiol. 232 (2017) 110–121, https://doi.org/10.1002/jcp.25395.

[31] I. Galve-Roperh, V. Chiurchiù, J. Díaz-Alonso, M. Bari, M. Guzmán, M. Maccarrone, Cannabinoid receptor signaling in progenitor/stem cell proliferation and differentiation, Prog. Lipid Res. 52 (2013) 633–650, https://doi.org/10.1016/j.plipres.2013.05.004.

[32] P. Morales, D.P. Hurst, P.H. Reggio, Molecular targets of the phytocannabinoids: a complex picture, Prog. Chem. Org. Nat. Prod. 103 (2017) 103–131, https://doi.org/10.1007/978-3-319-45541-9_4.

[33] V. Di Marzo, F. Piscitelli, The endocannabinoid system and its modulation by phytocannabinoids, Neurother. J. Am. Soc. Exp. Neurother. 12 (2015) 692–698, https://doi.org/10.1007/s13311-015-0374-6.

[34] A. Ligresti, L. De Petrocellis, V. Di Marzo, From phytocannabinoids to cannabinoid receptors and endocannabinoids: pleiotropic physiological and pathological roles through complex pharmacology, Physiol. Rev. 96 (2016) 1593–1659, https://doi.org/10.1152/physrev.00002.2016.

[35] E. D'Aniello, T. Fellous, F.A. Iannotti, A. Gentile, M. Allarà, F. Balestrieri, R. Gray, P. Amodeo, R.M. Vitale, V. Di Marzo, Identification and characterization of phytocannabinoids as novel dual PPARα/γ agonists by a computational and in vitro experimental approach, Biochim. Biophys. Acta Gen. Subj. 1863 (2019) 586–597, https://doi.org/10.1016/j.bbagen.2019.01.002.

[36] J. Díaz-Alonso, J. Paraíso-Luna, C. Navarrete, C. del Río, I. Cantarero, B. Palomares,

J. Aguareles, J. Fernández-Ruiz, M.L. Bellido, F. Pollastro, G. Appendino, M.A. Calzado, I. Galve-Roperh, E. Muñoz, VCE-003.2, a novel cannabigerol derivative, enhances neuronal progenitor cell survival and alleviates symptomatology in murine models of Huntington's disease, Sci. Rep. 6 (2016), https://doi.org/10.1038/srep29789.

[37] S. Valdeolivas, C. Navarrete, I. Cantarero, M.L. Bellido, E. Muñoz, O. Sagredo, Neuroprotective properties of cannabigerol in Huntington's disease: studies in R6/2 mice and 3-nitropropionate-lesioned mice, Neurother. J. Am. Soc. Exp. Neurother. 12 (2015) 185–199, https://doi.org/10.1007/s13311-014-0304-z.

[38] T. Stark, J. Ruda-Kucerova, F.A. Iannotti, C. D'Addario, R. Di Marco, V. Pekarik, E. Drazanova, F. Piscitelli, M. Bari, Z. Babinska, G. Giurdanella, M. Di Bartolomeo, S. Salomone, A. Sulcova, M. Maccarrone, C.T. Wotjak, Z. Starcuk, F. Drago, R. Mechoulam, V. Di Marzo, V. Micale, Peripubertal cannabidiol treatment rescues behavioral and neurochemical abnormalities in the MAM model of schizophrenia, Neuropharmacology 146 (2019) 212–221, https://doi.org/10.1016/j.neuropharm.2018.11.035.

[39] F.A. Iannotti, C.L. Hill, A. Leo, A. Alhusaini, C. Soubrane, E. Mazzarella, E. Russo, B.J. Whalley, V. Di Marzo, G.J. Stephens, Nonpsychotropic plant cannabinoids, cannabidivarin (CBDV) and cannabidiol (CBD), activate and desensitize transient receptor potential vanilloid 1 (TRPV1) channels in vitro: potential for the treatment of neuronal hyperexcitability, ACS Chem. Neurosci. 5 (2014) 1131–1141, https://doi.org/10.1021/cn5000524.

[40] A. Scutt, E.M. Williamson, Cannabinoids stimulate fibroblastic colony formation by bone marrow cells indirectly via CB2 receptors, Calcif. Tissue Int. 80 (2007) 50–59, https://doi.org/10.1007/s00223-006-0171-7.

[41] E. Schmuhl, R. Ramer, A. Salamon, K. Peters, B. Hinz, Increase of mesenchymal stem cell migration by cannabidiol via activation of p42/44 MAPK, Biochem. Pharmacol. 87 (2014) 489–501, https://doi.org/10.1016/j.bcp.2013.11.016.

[42] F.A. Iannotti, E. Pagano, A.S. Moriello, F.G. Alvino, N.C. Sorrentino, L. D'Orsi, E. Gazzerro, R. Capasso, E. De Leonibus, L. De Petrocellis, V. Di Marzo, Effects of non-euphoric plant cannabinoids on muscle quality and performance of dystrophic mdx mice, Br. J. Pharmacol. (2018), https://doi.org/10.1111/bph.14460.

[43] M. Tencerova, F. Figeac, N. Ditzel, H. Taipaleenmäki, T.K. Nielsen, M. Kassem, High-fat diet-induced obesity promotes expansion of bone marrow adipose tissue and impairs skeletal stem cell functions in mice, J. Bone Miner. Res. 33 (2018) 1154–1165, https://doi.org/10.1002/jbmr.3408.

[44] K. Kornicka, J. Houston, K. Marycz, Dysfunction of mesenchymal stem cells isolated from metabolic syndrome and type 2 diabetic patients as result of oxidative stress and autophagy may limit their potential therapeutic use, Stem Cell Rev. 14 (2018) 337–345, https://doi.org/10.1007/s12015-018-9809-x.

[45] E. Mansilla, V. Díaz Aquino, D. Zambón, G.H. Marin, K. Mártire, G. Roque, T. Ichim, N.H. Riordan, A. Patel, F. Sturla, G. Larsen, R. Spretz, L. Núñez, C. Soratti, R. Ibar, M. van Leeuwen, J.M. Tau, H. Drago, A. Maceira, Could metabolic syndrome, lipodystrophy, and aging be mesenchymal stem cell exhaustion syndromes? Stem Cells Int. (2011) 943216, https://doi.org/10.4061/2011/943216.

[46] F.A. Iannotti, E. Panza, V. Barrese, D. Viggiano, M.V. Soldovieri, M. Taglialatela, Expression, localization, and pharmacological role of Kv7 potassium channels in skeletal muscle proliferation, differentiation, and survival after myotoxic insults, J. Pharmacol. Exp. Ther. 332 (2010) 811–820, https://doi.org/10.1124/jpet.109.162800.

[47] F.A. Iannotti, E. Pagano, O. Guardiola, S. Adinolfi, V. Saccone, S. Consalvi, F. Piscitelli, E. Gazzerro, G. Busetto, D. Carrella, R. Capasso, P.L. Puri, G. Minchiotti, V. Di Marzo, Genetic and pharmacological regulation of the endocannabinoid CB1 receptor in Duchenne muscular dystrophy, Nat. Commun. 9 (2018) 3950, https://doi.org/10.1038/s41467-018-06267-1.

[48] X.-T. Feng, T.-Z. Wang, J. Leng, Y. Chen, J.-B. Liu, Y. Liu, W.-J. Wang, Palmitate contributes to insulin resistance through downregulation of the Src-mediated phosphorylation of Akt in C2C12 myotubes, Biosci. Biotechnol. Biochem. 76 (2012) 1356–1361, https://doi.org/10.1271/bbb.120107.

[49] P. Bianco, P.G. Robey, P.J. Simmons, Mesenchymal stem cells: revisiting history, concepts, and assays, Cell Stem Cell 2 (2008) 313–319, https://doi.org/10.1016/j.stem.2008.03.002.

[50] M. Patil, A. Patwardhan, M.M. Salas, K.M. Hargreaves, A.N. Akopian, Cannabinoid receptor antagonists AM251 and AM630 activate TRPA1 in sensory neurons, Neuropharmacology 61 (2011) 778–788, https://doi.org/10.1016/j.neuropharm.2011.05.024.

[51] Z. Cao, R.M. Umek, S.L. McKnight, Regulated expression of three C/EBP isoforms during adipose conversion of 3T3-L1 cells, Genes Dev. 5 (1991) 1538–1552, https://doi.org/10.1101/gad.5.9.1538.

[52] S. Nakamura, T. Tamura, N. Matsuzawa-Nagata, H. Takayama, H. Misu, H. Noda, S. Nabemoto, S. Kurita, T. Ota, H. Ando, K.-I. Miyamoto, S. Kaneko, Palmitate induces insulin resistance in H4IIEC3 hepatocytes through reactive oxygen species produced by mitochondria, J. Biol. Chem. 284 (2009) 14809–14818, https://doi.org/10.1074/jbc.M901488200.

[53] J.Y. Jeon, S.-E. Choi, E.S. Ha, H.B. Lee, T.H. Kim, S.J. Han, H.J. Kim, D.J. Kim, Y. Kang, K.-W. Lee, GLP-1 improves palmitate-induced insulin resistance in human skeletal muscle via SIRT1 activity, Int. J. Mol. Med. 44 (2019) 1161–1171, https://doi.org/10.3892/ijmm.2019.4272.

[54] J. Mo, Y. Zhou, R. Yang, P. Zhang, B. He, J. Yang, S. Li, Z. Shen, P. Chen, Ginsenoside Rg1 ameliorates palmitic acid-induced insulin resistance in HepG2 cells in association with modulating Akt and JNK activity, Pharmacol. Rep. 71 (2019) 1160–1167, https://doi.org/10.1016/j.pharep.2019.07.004.

[55] Q. Zhang, X. Kong, H. Yuan, H. Guan, Y. Li, Y. Niu, Mangiferin improved palmitate-induced-insulin resistance by promoting free fatty acid metabolism in HepG2 and C2C12 cells via PPARα: mangiferin improved insulin resistance, J. Diabetes Res. 2019 (2019) 2052675, https://doi.org/10.1155/2019/2052675.

[56] X. Chen, X. Zhao, F. Lan, T. Zhou, H. Cai, H. Sun, W. Kong, W. Kong, Hydrogen sulphide treatment increases insulin sensitivity and improves oxidant metabolism through the CaMKKbeta-AMPK pathway in PA-induced IR C2C12 cells, Sci. Rep. 7 (2017) 13248, https://doi.org/10.1038/s41598-017-13251-0.

[57] R. van Eenige, M. van der Stelt, P.C.N. Rensen, S. Kooijman, Regulation of adipose tissue metabolism by the endocannabinoid system, Trends Endocrinol. Metab. 29 (2018) 326–337, https://doi.org/10.1016/j.tem.2018.03.001.

[58] L. Cristino, T. Becker, V. Di Marzo, Endocannabinoids and energy homeostasis: an update, BioFactors Oxf. Engl. 40 (2014) 389–397, https://doi.org/10.1002/biof.1168.

[59] P.D. Cani, H. Plovier, M. Van Hul, L. Geurts, N.M. Delzenne, C. Druart, A. Everard, Endocannabinoids–at the crossroads between the gut microbiota and host metabolism, Nat. Rev. Endocrinol. 12 (2016) 133–143, https://doi.org/10.1038/nrendo.2015.211.

[60] N. Kim, S.-G. Cho, New strategies for overcoming limitations of mesenchymal stem cell-based immune modulation, Int. J. Stem Cells 8 (2015) 54–68, https://doi.org/10.15283/ijsc.2015.8.1.54.

[61] M. Garcia-Arencibia, E. Molina-Holgado, F. Molina-Holgado, Effect of endocannabinoid signalling on cell fate: life, death, differentiation and proliferation of brain cells, Br. J. Pharmacol. (2018), https://doi.org/10.1111/bph.14369.

[62] S.C. Dyall, H.K. Mandhair, R.E.A. Fincham, D.M. Kerr, M. Roche, F. Molina-Holgado, Distinctive effects of eicosapentaenoic and docosahexaenoic acids in regulating neural stem cell fate are mediated via endocannabinoid signalling pathways, Neuropharmacology 107 (2016) 387–395, https://doi.org/10.1016/j.neuropharm.2016.03.055.

[63] X. Nadal, C. Del Río, S. Casano, B. Palomares, C. Ferreiro-Vera, C. Navarrete, C. Sánchez-Carnerero, I. Cantarero, M.L. Bellido, S. Meyer, G. Morello, G. Appendino, E. Muñoz, Tetrahydrocannabinolic acid is a potent PPARγ agonist with neuroprotective activity, Br. J. Pharmacol. 174 (2017) 4263–4276, https://doi.org/10.1111/bph.14019.

[64] M.A. Deeg, M.H. Tan, Pioglitazone versus rosiglitazone: effects on lipids, lipoproteins, and apolipoproteins in head-to-head randomized clinical studies, PPAR Res. 2008 (2008) 520465, https://doi.org/10.1155/2008/520465.

[65] A. Krishnaswami, S. Ravi-Kumar, J.M. Lewis, Thiazolidinediones: a 2010 perspective, Perm. J. 14 (2010) 64–72.

[66] A. Taniguchi, M. Sakai, S. Teramura, M. Fukushima, K. Hama, K. Marumoto, N. Nezumi, T. Yoshida, S. Nagasaka, R. Hayashi, K. Tokuyama, Y. Nakai, Serum nonesterified fatty acids are related with carotid atherosclerotic plaque in nonobese nonhypertensive Japanese type 2 diabetic patients, Diabetes Care 24 (2001) 1505–1507.

[67] B. Grygiel-Górniak, Peroxisome proliferator-activated receptors and their ligands: nutritional and clinical implications – a review, Nutr. J. 13 (2014) 17, https://doi.org/10.1186/1475-2891-13-17.

[68] D. Moseti, A. Regassa, W.-K. Kim, Molecular regulation of adipogenesis and potential anti-adipogenic bioactive molecules, Int. J. Mol. Sci. 17 (2016), https://doi.org/10.3390/ijms17010124.

[69] M.I. Lefterova, A.K. Haakonsson, M.A. Lazar, S. Mandrup, PPARγ and the global map of adipogenesis and beyond, Trends Endocrinol. Metab. 25 (2014) 293–302, https://doi.org/10.1016/j.tem.2014.04.001.

[70] T. Shan, W. Liu, S. Kuang, Fatty acid binding protein 4 expression marks a population of adipocyte progenitors in white and brown adipose tissues, FASEB J. 27 (2013) 277–287, https://doi.org/10.1096/fj.12-211516.

[71] M. Eichler, L. Spinedi, S. Unfer-Grauwiler, M. Bodmer, C. Surber, M. Luedi, J. Drewe, Heat exposure of Cannabis sativa extracts affects the pharmacokinetic and metabolic profile in healthy male subjects, Planta Med. 78 (2012) 686–691, https://doi.org/10.1055/s-0031-1298334.

[72] I. Ujváry, L. Hanuš, Human metabolites of cannabidiol: a review on their formation, Biol. Activity Relevance Ther. Cannabis Cannabinoid Res. 1 (2016) 90–101, https://doi.org/10.1089/can.2015.0012.

[73] M. Mueckler, Insulin resistance and the disruption of Glut4 trafficking in skeletal muscle, J. Clin. Invest. 107 (2001) 1211–1213.

[74] L. Martinez, M. Berenguer, M.C. Bruce, Y. Le Marchand-Brustel, R. Govers, Rosiglitazone increases cell surface GLUT4 levels in 3T3-L1 adipocytes through an enhancement of endosomal recycling, Biochem. Pharmacol. 79 (2010) 1300–1309, https://doi.org/10.1016/j.bcp.2009.12.013.

[75] R. Berry, M.S. Rodeheffer, Characterization of the adipocyte cellular lineage in vivo, Nat. Cell Biol. 15 (2013) 302–308, https://doi.org/10.1038/ncb2696.

[76] F. Villarroya, R. Iglesias, M. Giralt, PPARs in the control of uncoupling proteins gene expression, PPAR Res. 2007 (2007) 74364, https://doi.org/10.1155/2007/74364.

[77] E. Hondares, M. Rosell, J. Díaz-Delfín, Y. Olmos, M. Monsalve, R. Iglesias, F. Villarroya, M. Giralt, Peroxisome proliferator-activated receptor α (PPARα) induces PPARγ coactivator 1α (PGC-1α) gene expression and contributes to thermogenic activation of brown fat: involvement of PRDM16, J. Biol. Chem. 286 (2011) 43112–43122, https://doi.org/10.1074/jbc.M111.252775.

[78] M.J. Barbera, A. Schluter, N. Pedraza, R. Iglesias, F. Villarroya, M. Giralt, Peroxisome proliferator-activated receptor alpha activates transcription of the brown fat uncoupling protein-1 gene. A link between regulation of the thermogenic and lipid oxidation pathways in the brown fat cell, J. Biol. Chem. 276 (2001) 1486–1493, https://doi.org/10.1074/jbc.M006246200.

[79] M. Alcalá, M. Calderon-Dominguez, D. Serra, L. Herrero, M. Viana, Mechanisms of impaired brown adipose tissue recruitment in obesity, Front. Physiol. 10 (2019) 94, https://doi.org/10.3389/fphys.2019.00094.

[80] T. Yamauchi, J. Kamon, Y. Minokoshi, Y. Ito, H. Waki, S. Uchida, S. Yamashita, M. Noda, S. Kita, K. Ueki, K. Eto, Y. Akanuma, P. Froguel, F. Foufelle, P. Ferre, D. Carling, S. Kimura, R. Nagai, B.B. Kahn, T. Kadowaki, Adiponectin stimulates

glucose utilization and fatty-acid oxidation by activating AMP-activated protein kinase, Nat. Med. 8 (2002) 1288–1295, https://doi.org/10.1038/nm788.

[81] R.J. Sulston, W.P. Cawthorn, Bone marrow adipose tissue as an endocrine organ: close to the bone? Horm. Mol. Biol. Clin. Invest. 28 (2016) 21–38, https://doi.org/10.1515/hmbci-2016-0012.

[82] L. Yu, Q. Tu, Q. Han, L. Zhang, L. Sui, L. Zheng, S. Meng, Y. Tang, D. Xuan, J. Zhang, D. Murray, Q. Shen, J. Cheng, S.-H. Kim, L.Q. Dong, P. Valverde, X. Cao, J. Chen, Adiponectin regulates bone marrow mesenchymal stem cell niche through a unique signal transduction pathway: an approach for treating bone disease in diabetes, Stem Cells Dayt. Ohio 33 (2015) 240–252, https://doi.org/10.1002/stem.1844.

[83] J.S. Hwang, W.J. Lee, J. Hur, H.G. Lee, E. Kim, G.H. Lee, M.-J. Choi, D.-S. Lim, K.S. Paek, H.G. Seo, Rosiglitazone-dependent dissociation of HuR from PPAR-γ regulates adiponectin expression at the posttranscriptional level, FASEB J. (2019), https://doi.org/10.1096/fj.201802643R fj201802643R.

[84] I. Barbagallo, G. Li Volti, F. Galvano, G. Tettamanti, F.R. Pluchinotta, S. Bergante, L. Vanella, Diabetic human adipose tissue-derived mesenchymal stem cells fail to differentiate in functional adipocytes, Exp. Biol. Med. Maywood NJ 242 (2017) 1079–1085, https://doi.org/10.1177/1535370216681552.

[85] A.S.I. Ahmed, M.H. Sheng, S. Wasnik, D.J. Baylink, K.-H.W. Lau, Effect of aging on stem cells, World J. Exp. Med. 7 (2017) 1–10, https://doi.org/10.5493/wjem.v7.i1.1.

[86] S. Bhansali, P. Dutta, V. Kumar, M.K. Yadav, A. Jain, S. Mudaliar, S. Bhansali, R.R. Sharma, V. Jha, N. Marwaha, N. Khandelwal, A. Srinivasan, N. Sachdeva, M. Hawkins, A. Bhansali, Efficacy of autologous bone marrow-derived mesenchymal stem cell and mononuclear cell transplantation in type 2 diabetes mellitus: a randomized, placebo-controlled comparative study, Stem Cells Dev. 26 (2017) 471–481, https://doi.org/10.1089/scd.2016.0275.

[87] P. Raskin, M. Rendell, M.C. Riddle, J.F. Dole, M.I. Freed, J. Rosenstock, Rosiglitazone Clinical Trials Study Group, A randomized trial of rosiglitazone therapy in patients with inadequately controlled insulin-treated type 2 diabetes, Diabetes Care 24 (2001) 1226–1232.

[88] M.J. Nanjan, M. Mohammed, B.R. Prashantha Kumar, M.J.N. Chandrasekar, Thiazolidinediones as antidiabetic agents: a critical review, Bioorgan. Chem. 77 (2018) 548–567, https://doi.org/10.1016/j.bioorg.2018.02.009.

[89] Y. Nishi, A. Murakami, Y. Murayama, N. Tsukahara, S. Okamoto, S. Nakachi, K. Morichika, K. Tamaki, H. Noguchi, M. Matsushita, K.-N. Karube, T. Fukushima, S. Morishima, H. Kishimoto, H. Masuzaki, Adipose tissue-derived mesenchymal stem cells ameliorate bone marrow aplasia related with graft-versus-host disease in experimental murine models, Transpl. Immunol. (2019), https://doi.org/10.1016/j.trim.2019.03.004.